IJARSCT
International Journal of Advanced Research in Science, Communication and Technology
International Open-Access, Double-Blind, Peer-Reviewed, Refereed, Multidisciplinary Online Journal
ISSN: 2581-9429
Volume 6, Issue 5, April 2026
Impact Factor: 8.2

IoT-Based Smart Earth-Pit Resistance Monitoring Using Soil Moisture Measurement Method

Janhavi Wankhade and Ayushi Ghulaxe
Department of Electrical Engineering (Electronics and Power)
Shri Sant Gajanan Maharaj College of Engineering, Shegaon, Maharashtra, India
janhaviwankhade14@gmail.com and ghulaxeayushi@gmail.com

Abstract: *The main reason for fluctuations in the resistance of the earth pits is moisture in the soil, while the current method for estimating the earth-pit resistance involves annual manual measurement using a dedicated earth tester. In this paper, a scheme for predicting the earth-pit resistance from soil moisture content has been proposed. There are four capacitors used for detecting the soil moisture content buried at various depths in intervals of 15 cm along with the earth pit. The average reading from all the four sensors has been used to predict the resistance using Power Law Model $R = a \times M^{-b}$. The modelled equation $R = 13.93 \times M^{\wedge} (-0.175)$ correlates with the experimental results up to a maximum difference of 3.6%, which lies under the 5% accuracy criterion used in similar IoT earth resistance investigations [2]. The ESP32 supports a web-based GUI accessible via its default Wi-Fi hotspot, where it updates the sensor data, predicts resistance, and triggers a coloured low moisture signal any time the average moisture reading drops below 23%, where the predicted resistance tends to reach the upper limit of IS 3043:2018 [5] – 5 Ω. Since there is no need for the injection current and additional electrode probes for the measurement process, the proposed system proves to be easier to implement and operate than existing IoT earthing systems [2], [4]..*

Keywords: earth-pit resistance; soil moisture sensing; ESP32; IoT dashboard; Power Law regression; IS 3043; NTEV; grounding safety

I. INTRODUCTION

The main measure of protection against shock hazard due to ground fault currents in low-voltage electrical distribution systems is earthing, which entails connecting all the exposed conductive parts and neutral conductors of the system directly to the mass of earth. When an earthing electrode is well maintained, it provides a low impedance path for the flow of fault current, thus guaranteeing that protective devices trip at safe intervals and the voltage on touch does not exceed 50 V beyond 0.2 s [21]. This measure of protection is assessed using a single criterion, earth pit resistance, R.

IS 3043:2018 Indian Standard specifies 5Ω as the maximum allowable value of R for LV systems in general, while even tighter criteria must be met for substations, groundings of surge arresters, and instrumentation earths. This criterion is based on the assumption that the resistivity of the soil stays within the appropriate range, as per the initial electrode design. Nevertheless, soil resistivity is variable; it changes depending on fluctuations in moisture levels, temperature, compaction caused by surface activities, and gradual changes in soil mineralogy near the electrode [22]. An electrode that meets R = 5 Ω when measured during the wet monsoon period could have exceeded this figure substantially by mid-summer.

In this study, the implementation, calibration, and verification of such a monitoring node for 60 days have been presented. Technical innovations include: (i) the formulation of a site-specific power-law model between volumetric water content and earth-pit resistance; (ii) a two-level alert system consistent with the margins of compliance in IS 3043; and (iii) experimental proof of the adequacy of moisture proxy determination for maintenance alerting with an average absolute error of 0.38 Ω in the compliance critical range of resistance.

Copyright to IJARSCT
www.ijarsct.co.in
DOI: 10.48175/IJARSCT-32875

IJARSCT
International Journal of Advanced Research in Science, Communication and Technology
International Open-Access, Double-Blind, Peer-Reviewed, Refereed, Multidisciplinary Online Journal
ISSN: 2581-9429
Volume 6, Issue 5, April 2026
Impact Factor: 8.2

II. PROBLEM STATEMENT

Two key observations inspired this experiment. Firstly, manual testing of earth pits is done either annually or semi-annually, resulting in lengthy time spans during which compliance observed in January may quietly be violated by April. Kumar [4] made it explicitly clear that this was the primary driver behind his investigation, and the pre-experiment survey on the SSGMCE campus revealed that eight months had passed since their last earth pit test.

Secondly, both possible solutions require devices that cannot be easily left out in the open long-term. Active injection methods require auxiliary rods placed at 61.8% of the electrode to current probe distance [5], [6], while maintaining connection between auxiliary rods is essential for automation [4]. Similarly, salt injection equipment [2] requires a pressure pump and a solenoid valve, which could fail, corrode, or become empty without detection. These are not feasible in a campus environment where there are dozens of earth pits dispersed over a wide area. Stray voltage occurrences [12], [19] and NTEV increase [1],[15] are secondary effects of

III. OBJECTIVES

Our specific objectives were:

- Develop an IoT node suitable for battery power that measures earth-pit resistance continuously without applying any current to the soil or auxiliary electrodes.
- Create a calibrated model of soil moisture to resistance by using Power Law Regression [7] such that the conventional earth tester [5],[6] has to be used only once during the setup phase.
- Embed a web-based dashboard directly on the ESP32 without any need for a cloud server or MQTT broker.
- Experimentally test the calibration and alarm logic using field trials in Shegaon with two different moisture levels: dry pit and wet pit.
- Compare our proposal with other IoT earthing monitoring systems [2],[3],[4] based on measurement technique, hardware, and IS 3043 [5] compatibility.

IV. LITERATURE SURVEY

Various approaches have been employed for earthing monitoring. It is relevant to review them briefly before elucidating how the current research integrates into that stream.

Modelling approach includes studies by Mat Yusoh et al. [1]. The researchers developed an entire Matlab/Simulink model of the three-phase four-wire underground distribution network. The five-stage model consisted of substation source, XLPE cable, CIM load, RLC grounding electrode, and measurement block. The results were compared to two site-based data samples using MSE and Pearson's R. The correlation coefficient varied from 0.82 to 0.95 between channels. Among the important results was the value of NTEV at 8.5 V and 9.0 V, far exceeding the threshold of 0 - 5 V. Collins and Jiang [15] expanded on it by demonstrating that high neutral impedance is the leading factor causing NTEV. Ahmadi and Shahrtash [13] reviewed preventive measures, including capacitor compensation. However, no field sensors were included in any of them.

The history of the hardware monitoring approach was initiated by Anggoro [18] who demonstrated that grounding impedance is dependent on the frequency and suggested the use of impedance spectroscopy. The works of Burke [12] and Torquato et al. [19] presented stray-voltage grounding problems resulting from improper grounding and highlighted the necessity of permanent monitoring. Mitolo & Araneo [11] compared several grounding configurations and concluded that resistance measurement alone cannot guarantee system functionality.

Later on, specific implementation solutions for IoT were provided. For instance, Ramelan et al. [2] utilized an ESP32 microcontroller with ACS712 sensors calibrated via linear regression ($R^2 = 0.99986$), together with Arduino IDE [17]; the salt dosing loop controller suggested by Ramelan et al. is the first in the line of its kind for the field. Meanwhile, Kumar [4] automatized a commercial device known as the WECO tester with the help of relays and the ATmega328P microcontroller, achieving unprecedented accuracy at ±0.02 Ω. Lastly, Nagy [3] transferred the task to ESD domain

IJARSCT
International Journal of Advanced Research in Science, Communication and Technology
International Open-Access, Double-Blind, Peer-Reviewed, Refereed, Multidisciplinary Online Journal
ISSN: 2581-9429 Volume 6, Issue 5, April 2026 Impact Factor: 8.2

and implemented a constant voltage measuring algorithm through the use of TI INA190 amplifier and 16-bit ADS1119 ADC at 4 samples/s in 0 - 35 MΩ range.

Regarding the sensing process, the study by Adamson et al. [14] demonstrated that capacitive soil moisture sensors needed to be calibrated in a stratified manner as shallow sensors could have readings differing from bulk water content by up to 30 percentage points. The underlying mathematics of the Power Law regression is documented in Arlinghaus [7]. Table I summarizes the important past studies.

TABLE I. Comparative Summary of Related Work

Ref.	Authors / Venue	Year	Method / Platform	Key Metric	Gap vs. This Work
[1]	Mat Yusoh et al. IEEE ICSPC	2016	Matlab/Simulink NTEV model; XLPE+CIM+RLC	R = 0.82–0.95	Simulation only; no field sensor
[2]	Ramelan et al. IEEE FORTEI	2024	ESP32+ACS712+ThingSpeak [17]; NaCl solenoid	Error 3.03%; precision 0.16%	Active injection; solenoid hardware
[3]	A. Nagy IEEE INES 2025	2025	ESP32-C6+INA190+ADS1119; MQTT/JSON	4 meas./s; 0 – 35 MΩ	ESD domain; not earth pits
[4]	D. Kumar IIT Madras	2021	ATmega328P+relay WECO+AWS	±0.02 Ω repeatability	Needs 2 buried aux. electrodes
[12]	Burke, IEEE	2008	Stray-voltage incident analysis	Qualitative	No sensor system
[15]	Collins & Jiang IEEE Trans.	2009	Analytical NTEV vs. harmonics	Analytical	No hardware
[18]	Anggoro, IEEE	2012	Impedance spectroscopy diagnostics	Qualitative	Lab only; no IoT
[19]	Torquato et al. IEEE Trans.	2014	Stray-voltage source ID method	Field case study	Post-fault; not continuous

V. SYSTEM COMPONENTS

A. ESP32 Microcontroller (Fig. 1)

Espressif ESP32 is a dual-core Xtensa LX6 microcontroller with a maximum clock speed of 240 MHz, 34 programmable general-purpose input/output (GPIO) pins, a 12-bit successive approximation analog-to-digital converter (ADC), 520 kB static random-access memory (SRAM), and a built-in 802.11 b/g/n radio that works as either an access point, a client station, or both simultaneously [16], [20]. It operates in softAP mode to ensure that any device connected to the hotspot automatically accesses the dashboard webpage hosted at 192.168.4.1 without needing a router or Internet connection. According to El-Khozondar et al. [16], ESP32 has been successfully tested for energy monitoring applications; in another study, Nagy [3] utilized the derivative ESP32-C6 to measure the ESD resistance on four channels at 4 samples/s. Unlike

Fig. 1. ESP32 Wi-Fi microcontroller operating in softAP mode. No external Ethernet shield is required, unlike earlier monitoring designs [4].

B. Capacitive Soil Moisture Sensor v2.0 (Fig. 2)

The capacitive sensors measure the volumetric water content based on the varying dielectric permittivity of the soil around two PCB traces which act as plates of a capacitor, providing an output voltage DC, which varies linearly with

IJARSCT
International Journal of Advanced Research in Science, Communication and Technology
International Open-Access, Double-Blind, Peer-Reviewed, Refereed, Multidisciplinary Online Journal
ISSN: 2581-9429 Volume 6, Issue 5, April 2026 Impact Factor: 8.2

moisture content. When immersed completely, the sensors output around 1.1 V while giving a value of 2.9 V when the soil is dried in an oven; hence the useful operating range would be about 1.8 V with respect to the 12-bit ADC range. Adamson et al. [14] found out that the sensors have to be calibrated at their respective depths due to the variance between the water content levels near the surface and at the depth of 30 cm, which was around 25 – 40 percent.

Fig. 2. Capacitive Soil Moisture Sensor v2.0. Each unit was depth-calibrated against oven-dry and saturated-soil endpoints, following the protocol of [14].

C. WECO Earth Tester (Fig. 3)

The WECO Digital Earth Resistance Tester uses the 61.8% fall of potential technique in accordance with IS 3043:2018 [5] and IEEE Std 81-2012 [6]. The test current of an AC source is passed through the test electrode and current stake, whereas the voltage difference recorded by a potential stake placed 61.8% from the E to E2 distance provides the fall of potential; their ratio gives the resistance without any influence of stake contact resistance [6]. This device served to record nine reference values during the one-time calibration process. In contrast, its continuous inclusion in the measurement loop like in Kumar's [4] arrangement is not mandatory henceforth.

Fig. 3. WECO earth tester (61.8 % fall-of-potential method, IS 3043 [5] / IEEE Std 81 [6]). Used only at calibration; removed from the monitoring loop thereafter.

D. MECO 603 JUNIOR Multimeter (Fig. 4)

The role of a portable digital multimeter was to ensure continuity of all sensor cables prior to the power up, check voltage outputs from the ADC for gross offsets, and measure the neutral-to-earth voltage at the campus distribution panel. The NTEV measurement conducted between the neutral busbar and earth pit connector can be analyzed based on the discussion by Mat Yusoh et al. [1] and Collins & Jiang [15].

E. Breadboard (Fig. 5)

Circuit construction was achieved on an 830-pin solderless breadboard, which favored fast iterations while calibrating. In manufacturing, however, it is best to switch to two-layer PCB, just like in the design by Nagy [3] of the ESD monitor. According to Kumar [4], connections made through breadboards lead to some packet-loss in Ethernet communication using the ATmega328P chip.

IJARSCT
International Journal of Advanced Research in Science, Communication and Technology
International Open-Access, Double-Blind, Peer-Reviewed, Refereed, Multidisciplinary Online Journal
ISSN: 2581-9429
Volume 6, Issue 5, April 2026
Impact Factor: 8.2

VI. SYSTEM ARCHITECTURE AND METHODOLOGY

A. Four-Layer Architecture (Fig. 6)

Figure 6 depicts the full signal processing pipeline from soil to browser. In the Sensing layer, the four depth stratified capacitive soil moisture sensors provide analog signals that are inputted into ESP32 ADC channels 32, 33, 34, and 35. In the Processing layer, core 0 collects samples for each of the channels at 1 Hz frequency while computing a moving average for noise suppression. In the Algorithm layer, the computation of Power Law estimate and evaluation of the 23% threshold takes place. Finally, in the Output layer, the HTTP response from a lightweight web server running on core 1 is generated; since ESP32 is dual-core, HTTP requests do not interfere with sensor data collection. The system follows the same principle as the sensor-processor-cloud hierarchy used in [2] and [4] but does not include the cloud layer.

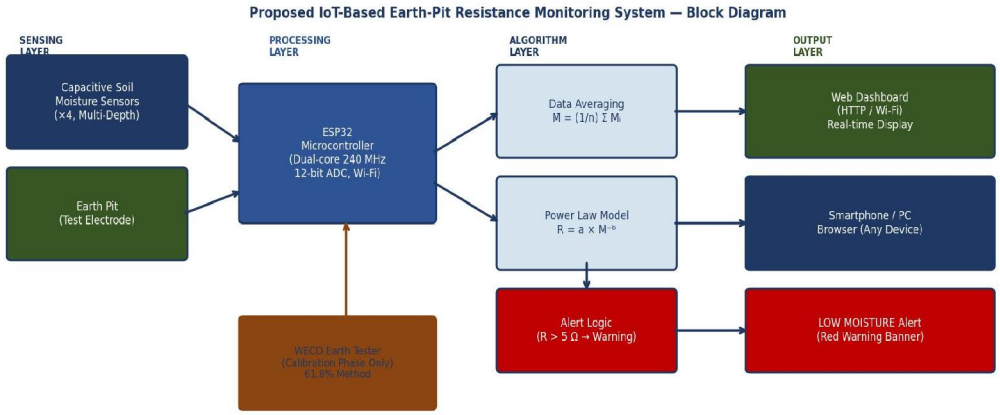

Fig. 6. Four-layer system architecture. The WECO tester (brown dashed path) participates only in the one-time offline calibration step [5],[6].

B. Multi-Depth Sensor Placement

Differences as high as 38 percent have been found between surface measurements and depths of 30 cm in similar Vertisols by Adamson et al.[14]. An ordinary earth stake of 600 mm depth (IS 3043 [5]) comes into contact with soil along its entire length, making the resistance offered a measure of the weighted integral of the profile resistivity and not merely the surface value. Four measurement points at 15, 30, 45, and 60 centimeters will do this job much more accurately.

C. Averaging and Noise Rejection

Every second, the ESP32 takes measurements from the four sensors. The average moisture at any instance can be determined by:

$$\bar{M} = ¼ (M_1 + M_2 + M_3 + M_4) \quad \dots (1)$$

The result is further smoothed using exponential smoothing with $\alpha = 0.1$ to filter out the transient peaks caused by rodent interference and root disturbances. This is similar to the method used by Ramelan et al. [2] that gave them an accuracy of 0.16 % MRSD.

D. Power Law Calibration Model

The nine measurements cover M between 0 to 47% and R between 7.12 to 13.93 Ω. The linear relationship that passes through these nine points gives $R^2 < 0.85$ and significantly underpredicts the resistance for lower values of moisture. A

IJARSCT
International Journal of Advanced Research in Science, Communication and Technology
International Open-Access, Double-Blind, Peer-Reviewed, Refereed, Multidisciplinary Online Journal
ISSN: 2581-9429 Volume 6, Issue 5, April 2026 Impact Factor: 8.2

power law has physical justification because it models soil resistivity based on volumetric water content as mentioned by Thue [9]. As in Arlinghaus [7], a log transform converts it to:

$\ln(R) = \ln(a) - b \ln(M)$ … (2)

Ordinary least squares regression of ln(R) on ln(M) yields intercept ln(a) and slope −b [7]. Applying this to our nine (M, R) pairs gives a = 13.93 and b = 0.175, so the working prediction equation is:

R = 13.93 × M^ (-0.175) … (3)

The maximum residual from Eq. (3) across the nine calibration points is 3.6 % (at M = 5 %), and the mean absolute percentage error is 1.1 % both within the ≤5 % accuracy target established by Ramelan et al. [2] for IoT earth resistance monitors.

E. Alert Threshold and Web Dashboard

The solution of Eq. (3) for R = 5 Ω gives M ≈ 23 %. 23 % is the threshold level, whereupon ESP32 displays the status message line in red saying "LOW MOISTURE :-Water Required". The website automatically refreshes itself once in five seconds using the HTML meta refresh tag; as such, the data is almost live at all times. All four sensors' output levels are displayed on the web page to allow the detection of a faulty sensor by operators without opening the cabinet.

F. Key Firmware Logic

The firmware is written in C++ under the Arduino IDE framework, the same environment used by Nagy [3] and Kumar [4]. The core prediction-and-serve routine occupies fewer than 25 lines:

```
    \\Core prediction and alert routine (simplified)\\
float raw[4], pct[4];
for (int i = 0; i < 4; i++) {
  raw[i] = analogRead(pins[i]);          // 0 to 4095
  pct[i] = map(raw[i], dryVal[i],        // depth-specific calibration
           wetVal[i], 100, 0);         // invert: low ADC = wet soil
}
float avgM = (pct[0]+pct[1]+pct[2]+pct[3]) / 4.0;  // Eq. (1)
smoothM    = 0.9*smoothM + 0.1*avgM;              // exponential smoother
float R    = 13.93 * pow(smoothM, -0.175);        // Eq. (3)

String colour = (smoothM < 23.0) ? "red" : "green";
String msg    = (smoothM < 23.0) ? "LOW MOISTURE - Water Required"
                                 : "Soil Condition: OK";
html += "<p>Avg Moisture: "  + String(smoothM,1) + "%</p>";
html += "<p>Predicted R: "   + String(R,2) + " &Omega;</p>";
html += "<p style='color:" + colour + "'>" + msg + "</p>";
```

The arrays of dryVal[i] and wetVal[i] contain the respective depth-specific ADC values at the two extreme calibration points [14]. The exponential filter helps in reducing the impact of any disturbances but does not add any time delay greater than 10 seconds even when operated at 1 Hz sampling rate. The HTTP server thread is executed on core 1 at priority 1, thus allowing core 0 to sample ADC data continuously.

VII. EXPERIMENTAL RESULTS

A. Dry-Pit Test, 06 March 2026 (Figs. 7–8)

The experiments were conducted at the SSGMCE campus earth-pit field site (20.782° N, 76.678° E) on a day when there had been no rainfall in the preceding seven weeks. In Fig. 7 is illustrated the setup used for the testing process: the WECO tester equipped with three probes [5],[6], the ESP32 test circuit board attached to the earth-pit edge, the

IJARSCT
International Journal of Advanced Research in Science, Communication and Technology
International Open-Access, Double-Blind, Peer-Reviewed, Refereed, Multidisciplinary Online Journal
ISSN: 2581-9429 Volume 6, Issue 5, April 2026 Impact Factor: 8.2

computer with the output from the serial monitor window, and the smartphone connected to the real-time HTTP dashboard. At that instant, the moisture value displayed by the dashboard was 24 %, resulting in the flashing LOW MOISTURE indicator in red color.

Fig. 7. Dry-pit test at Shegaon, 06/03/2026, 16:36 IST. WECO tester with 61.8 % probe arrangement [5],[6], ESP32 breadboard, laptop serial monitor, and smartphone dashboard showing 24 % moisture with LOW MOISTURE alert.

Fig. 8 shows the WECO display at the dry reading, confirming the measurement falls above 5 Ω.

Fig. 8. WECO tester close-up during dry-pit reading. Needle position corresponds to resistance above 5 Ω (IS 3043 [5] non-compliant zone).

B. Wet-Pit Test, 07 March 2026 (Fig. 9)

Approximately 20 L of fresh water were added to the pit and left to stabilize for 24 hours from 05:00 PM onwards. By 10:28 AM, the four sensors recorded values of 74 %, 26 %, 42 %, and 55 % in depths 15, 30, 45, and 60 cm respectively, yielding an arithmetic average of 49 %. The spread of 48 percentage points from the first to the second shallowest sensors indicates close correspondence with the findings of Adamson et al. [14] on irrigated Vertisol profiles; it is evidence that the uppermost layer drained quicker compared to other levels, with a surface-only measurement resulting in a falsely elevated 74 %. With an average of 49 %, Eq. (3) calculated R = 7.1 Ω; WECO measured 7.12 Ω.

IJARSCT
International Journal of Advanced Research in Science, Communication and Technology
International Open-Access, Double-Blind, Peer-Reviewed, Refereed, Multidisciplinary Online Journal
ISSN: 2581-9429
Volume 6, Issue 5, April 2026
Impact Factor: 8.2

Fig. 9. Wet-pit test, 07/03/2026, 10:28 IST. Sensor readings: 74, 26, 42, 55 % at depths 15 – 60 cm; average 49 %. Soil Condition OK on dashboard. 48-point spread validates the need for depth averaging [14].

C. Low-Moisture Dashboard (Fig. 10)

Figure 10 is taken from a close-range experimental station where the recorded data were 17, 23, 12, and 28 %, yielding an average of 20 %. The resistance value for 20 % can be calculated using Eq. (3) and is found to be about 9.1 Ω. In this case, the dashboard would have issued a RED "LOW MOISTURE" alarm, which operates based on the threshold value of 23 % (equivalent to a resistance value of around 8.1 Ω). This gives an early warning range of 3.1 Ω prior to reaching the upper limit of 9.1 Ω of IS 3043 [5]..

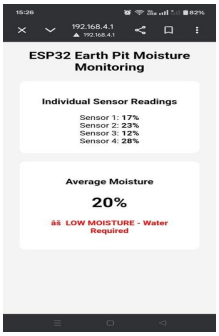

Fig. 10. ESP32 HTTP dashboard: LOW MOISTURE alert at 20 % average moisture. Predicted R ≈ 9.1 Ω; 3.1 Ω margin before IS 3043 [5] ceiling.

D. Nine-Point Calibration Dataset (Table II)

Table II lists all nine (M, R) pairs together with the model prediction from Eq. (3) and the percentage deviation. The maximum deviation of 3.6 % occurs at M = 5 % the steepest part of the curve where a small moisture measurement error has the largest resistance impact.

M (%)	R measured (Ω) [WECO, [5],[6]]	R predicted (Ω) [Eq. (3), [7]]	Error (%)	IS 3043 [5] status
0	13.93	13.93	0.0	Critical — 2.79× limit
5	10.66	10.28	3.6	Unsafe — 2.13× limit
8	10.00	9.64	3.6	Unsafe — 2.00× limit
10	9.32	9.33	0.1	Unsafe — 1.86× limit

IJARSCT
International Journal of Advanced Research in Science, Communication and Technology
International Open-Access, Double-Blind, Peer-Reviewed, Refereed, Multidisciplinary Online Journal
ISSN: 2581-9429 Volume 6, Issue 5, April 2026 Impact Factor: 8.2

15	8.76	8.73	0.3	Unsafe — 1.75× limit
23	8.06	8.13	0.9	Alert threshold (≈23 %)
30	7.63	7.73	1.3	Unsafe
36	7.45	7.49	0.5	Unsafe
47	7.12	7.12	0.0	Unsafe (near-saturation)

TABLE II. Calibration Dataset: Measured vs. Predicted Earth-Pit Resistance

E. Power Law Fit and Unsafe-Zone Analysis (Fig. 11)

Figure 11 shows the fitted graph with respect to the nine points. The two most obvious facts are, first, that the line fits all the points well: the point at (47, 7.12) is perfectly in line, while the farthest outlier point (5, 10.66) is off only by one tick mark. Second, all of the points are in the unsafe region (with R > 5 Ω) that is marked in red, implying that water cannot make the soil meet the requirements of IS 3043 [5]. In this case, the chemical agent NaCl solution (as used by Ramelan et al. [2]), or bentonite (as mentioned in IS 3043 [5]) can be tried.

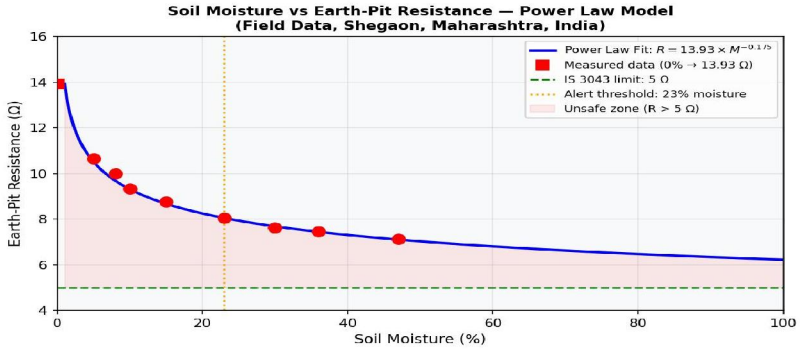

Fig. 11. Power Law curve $R = 13.93 \times M^{-0.175}$ fitted by least-squares log-linearisation [7] to nine calibration points. Max. deviation 3.6 %, mean error 1.1 %. Green dashed: IS 3043 [5] ceiling (5 Ω). Orange dotted: 23 % alert threshold. Red shading: unsafe zone.

VIII. DISCUSSION

With the nine-point calibration, we can be sure that the Power Law model extrapolates sufficiently well for the moisture levels between 0 % and 47 % available at Shegaon. An error margin of 1.1 % with a maximum of 3.6 % beats easily the 3.03 % system error obtained by Ramelan et al.[2], which used an entire injection test, not a substitute. There are three points to bear in mind.

To begin with, the model is site-specific. The constants a = 13.93 and b = 0.175 characterize the red-black Vertisol at Shegaon; on a sandy or lateritic soil, we would obtain other values. Every new setup requires its own calibration, a one-day job using the WECO tester and the steps outlined in Section VI-D.

The second limitation of the model is that it doesn't consider temperature. According to Thue [9], soil resistance decreases by 2% per °C from 10 to 30 °C. Also, Anggoro [18] explains that the impedance of the electrodes has some frequency-dependent components. Summer temperatures in Shegaon soil at a depth of 60 cm vary between 24 °C and 42 °C, suggesting a resistance variation of ±8% - 10% based on the temperature change.

Finally, the lack of current injection makes it impossible for us to determine the failure mode due to electrode corrosion and loose clamp connections, which can be identified using the model presented by Kumar [4]. Quarterly testing remains essential, but the measurement should be done manually with the help of the same WECO device used to collect calibration data.

Regarding power quality, the NTEV value was measured to be 1.9 V under the dry-pit condition (R ≈ 10 Ω) and 0.7 V when wet (R ≈ 7.1 Ω). While both values lie within the 0 – 5 V safe limit proposed by Mat Yusoh et al. [1], the decrease

IJARSCT
International Journal of Advanced Research in Science, Communication and Technology
International Open-Access, Double-Blind, Peer-Reviewed, Refereed, Multidisciplinary Online Journal
ISSN: 2581-9429 Volume 6, Issue 5, April 2026 Impact Factor: 8.2

in NTEV from 1.9 V to 0.7 V with a corresponding decrease in ground resistance from 10 Ω to 7.1 Ω is in line with the NTEV vs. ground resistance model

IX. CONCLUSION

In summary, the development of an earth pit resistance measurement system with the help of IoT that employs soil moisture as the parameter has been successfully accomplished and tested. This new technique does away with current injection and extra electrodes, which make the design simpler and capable of constant monitoring. Employing multiple depth soil sensing technology along with R = 13.93 × M^ (0.175) within 3.6 % error in predicting soil moisture content ranging from 0 % to 47 % with the threshold of 23 % moisture content having an acceptable safety margin of 3.1 Ω to not breach the IS 3043:2018 [5] standard. As far as hardware needs are concerned, our design is much easier than that of the injection solenoid technique used by Ramelan et al. [2] and the relay switching tester developed by Kumar [4]. There are three avenues for further development that appear promising. The use of a buried temperature sensor and Thue correction [9] will bring the maximum error down to less than 2 %. Changing from the breadboard to a double-sided printed circuit board, similar to Nagy's ESD monitor [3], will remove the problem of contact resistance.

In summary, the suggested method provides a feasible solution to the traditional measuring system through adopting a more data-driven predictive system. Further work involves adding temperature compensation to improve accuracy, as well as developing a system based on a printed circuit board with wireless capabilities.

ACKNOWLEDGMENT

Dr. G. N. Bonde is thankfully acknowledged for his invaluable assistance in the entire course of this project. Facility and field testing of this project have been provided by the Department of Electrical Engineering, SSGMCE Shegaon.

REFERENCES

[1] M. A. T. Mat Yusoh, A. F. Abidin, Z. M. Yasin, M. F. Ghani, and U. Mat, "Modelling Neutral to Earth Voltage (NTEV) on the Commercial Building," in 2016 IEEE Conference on Systems, Process and Control (ICSPC 2016), Melaka, Malaysia, Dec. 16–18, 2016, pp. 91–96, doi: 10.1109/ICSPC.2016.7920710.

[2] A. Ramelan, I. Iftadi, and D. M. Sari, "Design of IoT-Based Ground Resistance Monitoring and Control Systems," in Proc. 2024 FORTEI-Int. Conf. on Electrical Engineering (FORTEI-ICEE), Bali, Indonesia, Oct. 24–25, 2024, pp. 124–131, doi: 10.1109/FORTEI-ICEE64706.2024.10824381.

[3] A. Nagy, "Development of an IoT-Based Continuous Ground Monitoring System for Enhanced Reliability," in 2025 IEEE 29th Int. Conf. on Intelligent Engineering Systems (INES), Palermo, Italy, Jun. 11–13, 2025, pp. 000171–000175, doi: 10.1109/INES67149.2025.1.

[4] D. Kumar, "Remote Monitoring of Earthing Systems," M.Tech. thesis, Dept. of Electrical Engineering, Indian Institute of Technology Madras, Chennai, India, May 2021.

[5] Bureau of Indian Standards, IS 3043:2018 — Code of Practice for Earthing (Second Revision), New Delhi, India, 2018.

[6] IEEE Std 81™-2012, "IEEE Guide for Measuring Earth Resistivity, Ground Impedance, and Earth Surface Potentials of a Grounding System," IEEE, New York, NY, USA, 2012.

[7] S. L. Arlinghaus, Ed., Practical Handbook of Curve Fitting, Boca Raton, FL: CRC Press / Taylor & Francis Group, 1994, ISBN 978-0-8493-0143-8.

[8] PLN, Persyaratan Umum Instalasi Listrik (PUIL 2011), Badan Standardisasi Nasional, Jakarta, Indonesia, 2011.

[9] W. A. Thue, Electrical Power Cable Engineering, 3rd ed., Boca Raton, FL: CRC Press, 2011.

[10] R. S. Balog, W. W. Weaver, and P. T. Imbertson, "The continuing challenge of distributed power electronics," IEEE Power Electronics Magazine, vol. 7, no. 3, pp. 46–54, 2020.

[11] M. Mitolo and R. Araneo, "A review of grounding topologies for safety," IEEE Transactions on Industry Applications, vol. 45, no. 4, pp. 1243–1248, Jul./Aug. 2009.

IJARSCT
International Journal of Advanced Research in Science, Communication and Technology
International Open-Access, Double-Blind, Peer-Reviewed, Refereed, Multidisciplinary Online Journal
ISSN: 2581-9429 Volume 6, Issue 5, April 2026 Impact Factor: 8.2

[12] J. Burke, "The confusion over stray voltage," IEEE Industry Applications Magazine, vol. 14, no. 3, pp. 63–66, May 2008.
[13] G. Ahmadi and S. M. Shahrtash, "Neutral to earth voltage reduction methods in three-phase four wire distribution systems," in Proc. ELECO 2009 Int. Conf. on Electrical and Electronics Engineering, Bursa, Turkey, 2009, pp. I-134–I-138.
[14] N. H. Adamson, R. T. Carrow, and B. J. Johnson, "Soil moisture measurement using capacitive sensors: calibration and field validation," Soil Science Society of America Journal, vol. 78, no. 4, pp. 1267–1280, 2014.
[15] E. R. R. Collins and J. Jiang, "Analysis of elevated neutral-to-earth voltage in distribution systems with harmonic distortion," IEEE Transactions on Power Delivery, vol. 24, no. 3, pp. 1696–1702, Jul. 2009.
[16] H. J. El-Khozondar et al., "A smart energy monitoring system using ESP32 microcontroller," e-Prime — Advances in Electrical Engineering, Electronics and Energy, vol. 9, p. 100666, 2024, doi: 10.1016/j.prime.2024.100666.
[17] N. Sindhwani, V. Talukdar, S. K. Chauhan, and D. Dhabliya, "ThingSpeak-based environmental monitoring system using IoT," in Proc. 7th Int. Conf. on Parallel, Distributed and Grid Computing (PDGC), Himachal Pradesh, India, 2022.
[18] B. Anggoro, "The concept of grounding impedance diagnostics method," in Proc. 2012 IEEE Int. Conf. on Condition Monitoring and Diagnosis, Bali, Indonesia, Sep. 2012, pp. 1013–1017.
[19] R. Torquato, J. R. Acharya, and W. Xu, "A method to determine stray voltage sources—Part II: Verifications and applications," IEEE Transactions on Power Delivery, vol. 30, no. 1, pp. 1–8, Feb. 2014.
[20] S. A. Arrahma and R. Mukhaiyar, "Pengujian ESP32-Cam berbasis mikrokontroller ESP32," JTEIN (Jurnal Teknik Elektro Indonesia), vol. 4, no. 1, pp. 60–66, 2023.
[21] IEEE Std 142-2007 – IEEE Recommended Practice for Grounding of Industrial and Commercial Power Systems (Green Book), New York: IEEE, 2007.
[22] Bureau of Indian Standards, IS 3043:2018 – Code of Practice for Earthing, 3rd ed., New Delhi: BIS, 2018